Age of Information Minimization for Frameless ALOHA in Grant-Free Massive Access

Yuhao Huang, Jian Jiao, *Senior Member, IEEE*, Ye Wang, *Member, IEEE*, Xingjian Zhang, *Member, IEEE*, Shaohua Wu, *Member, IEEE*, Rongxing Lu, *Fellow, IEEE*, and Qinyu Zhang, *Senior Member, IEEE*

***Abstract*— In this paper, we focus on the optimal problem of average age of information (AAoI) in grant-free massive access, and propose an age-critical frameless ALOHA (ACFA) random access protocol, where the AAoI is implicitly reduced by banning the transmission of activated user equipments (UEs) recovered successfully in the last frame. In particular, we analyze the dense and sparse access models according to the activation probability, and present these scenarios with time-stamped sampling either at the beginning of the frame or in the first slot transmitting the packet. In order to qualify the AAoI of proposed protocol, we define two virtual rates and establish an iterative framework to analyze the access successful probability (ASP) of the protocol in asymptotic regime, and derive the closed-form expressions of AAoI as a function of ASP and virtual rate in all cases. Further, we formulate the optimal problems of normalized AAoI in all cases, and obtain the selection of access parameters by asymptotic analysis and simulations, respectively. Finally, we compare our protocol with state-of-the-art schemes, and the simulation results show that the ACFA random access protocol outperforms these benchmark schemes, and has great potential of access-banned policy in minimizing AAoI for frame-based protocols.**

***Index Terms*— Age of information, access policy, massive access, grant-free, frameless ALOHA.**

I. Introduction

MASSIVE machine-type communication (mMTC) is the most important scenario for future Internet of Things (IoT), and aspires to support the sporadic burst access, where massive number of uesr equipments (UEs) activate and transmit packets to the base station (BS) over a common shared channel [1], [2]. For the IoT UEs with low computing capabilities, the traditional 4-step access scheme (e.g. NR) needs to be simplified to adapt to mMTC service, and the grant-free protocols are proposed with the 2-step access process and simpler configurations to reduce the complexity and delay [3], [4].

A type of grant-free protocol is represented by the slotted ALOHA protocol [5], where the processing complexity and delay are reduced. Since there is no conflict detection, there is a high collision probability between packets, which can only reach $1/e$ of normalized throughput under high load conditions. In order to break through the performance bottleneck of the above protocols, a new frame-based grant-free access protocol using successive interference cancellation (SIC) technology is proposed, which is called code slotted ALOHA (CSA) protocol [6], [7], [8], [9], [10], [11]. Among them, the frameless ALOHA (FA) protocol is a simple CSA protocol, where UEs transmit the replicas of the packets with a constant probability (called access probability) on each slot in a frame, and the BS utilizes the SIC to decode the packets, which is similar to the belief propagation (BP) decoding of the LT code in binary erasure channel (BEC) [12]. The finite-length performance of FA protocol is analyzed in [13], showing that it is a simple but throughput-efficient protocol. While the performance of CSA protocol, especially the FA protocols are mainly determined by the access parameters, so the performance of active UE detection is also critical [14], [15].

On the other hand, in some typical IoT scenarios, e.g., in wireless sensor network (WSN), sensor nodes transmit monitoring indicators to information fusion nodes in real time, which puts forward higher requirements for the system freshness [16]. How to measure and improve the freshness of the system has become a key problem that need to be solved urgently [17]. At present, researchers use a new metric called age of information (AoI) to describe the freshness of packets monitored by UEs in mMTC scenarios, which originated from [18]. AoI is related to the time-stamp interval between two update packets transmit by UE, and BS calculates the average AoI (AAoI) to get the freshness description of the system by fairly measuring the AoI of all UEs [19]. It should be noted that AoI is different from other traditional indicators, e.g., delay, which has been verified in some works [17], [18], [19].

A class of fundamental works has gained attention, deriving the closed expressions of AAoI in CSA protocols [20], [21], [22], [23]. In [23], the authors further discuss the gain of AAoI brought by the SIC process early in the frame, and

Manuscript received 22 November 2022; revised 11 March 2023; accepted 25 April 2023. Date of publication 11 May 2023; date of current version 12 December 2023. This work was supported in part by the National Natural Sciences Foundation of China (NSFC) under Grant 62071141, Grant 61871147, Grant 61831008, and Grant 62027802; in part by the Shenzhen Science and Technology Program under Grant JSGG20220831110801003 and Grant GXWD20201230155427003-20200822165138001; and in part by the Major Key Project of PCL Department of Broadband Communication. The associate editor coordinating the review of this article and approving it for publication was S. Zhou. *(Corresponding authors: Jian Jiao; Qinyu Zhang.)*

Yuhao Huang, Jian Jiao, Xingjian Zhang, Shaohua Wu, and Qinyu Zhang are with the Guangdong Provincial Key Laboratory of Aerospace Communication and Networking Technology, Harbin Institute of Technology at Shenzhen, Shenzhen 518055, China, and also with the Peng Cheng Laboratory, Shenzhen 518055, China (e-mail: 20s152118@stu.hit.edu.cn; jiaojian@hit.edu.cn; x.zhang@hit.edu.cn; hitwush@hit.edu.cn; zqy@hit.edu.cn).

Ye Wang is with the Peng Cheng Laboratory, Shenzhen 518055, China (e-mail: wangy02@pcl.ac.cn).

Rongxing Lu is with the Faculty of Computer Science (FCS), University of New Brunswick (UNB), Fredericton, NB E3B 5A3, Canada (e-mail: rlu1@unb.ca).

Color versions of one or more figures in this article are available at https://doi.org/10.1109/TWC.2023.3273531.

Digital Object Identifier 10.1109/TWC.2023.3273531

obtain the corresponding optimal degree distribution based on the asymptotic regime analysis. However, these works focus on giving closed expressions of AAoI in the CSA protocols without redesigning a new access policy based on the AoI characteristics.

Another category of works is based on the slotted ALOHA protocol, which discussed the impact of the arrival rate and packet error rate (PER) to the system AoI [24], and redesign the age-related random access policy [25], [26], [27], [28]. The authors in [25] find that the AAoI can be effectively reduced, when the UE can access only if the AoI is greater than a certain threshold. The authors in [26] and [27] conduct a comprehensive steady-state analysis of the threshold ALOHA protocol, and obtain the corresponding AoI expressions, which can optimize the access parameters of the protocol. The authors in [28] study the slotted ALOHA protocol with a fixed and adaptive thresholds, respectively, and derive the lower bounds.

Therefore, we propose an access-banned policy with a threshold policy to improve the AAoI performance of the CSA protocol [29], and extend to the dense and sparse access models with two sampling methods. We reveal how the access-banned policy affects the AAoI performance of the FA protocol, further supporting its use in mMTC scenarios. Then, we analyze the theoretical performance of the corresponding access models and AoI sampling methods, and innovatively propose the age-critical frameless ALOHA (ACFA) random access protocol to ensure higher throughput while minimize the AAoI. Our contributions are summarized as follows.

- We propose the ACFA random access protocol, which improves the overall AAoI performance by banning the access of UEs that have been decoded successfully in the previous frame. According to different access requirements of mMTC scenarios, we subdivided into dense and sparse access models according to the active probability of UEs. Then, we introduce the AoI to measure the information freshness of the whole system, and two AoI sampling methods are subdivided at the sender according to the characteristics of the mMTC service.
- In order to analyze the AAoI performance of the proposed protocol, we distinguish the active UE and the access UE, and define two virtual code rates to track the trend of the number of allowed-access UEs in each frame, and then establish an iterative framework for the access successful probability (ASP) of the ACFA random access protocol in the asymptotic regime in two access models, respectively. Note that this iterative framework can analyze the ASP of all CSA protocol under the access-banned policy. We derive the closed-form expressions of the AAoI as a function with virtual code rates and ASP in two access models and two sampling methods, respectively.
- Finally, we propose four normalized AAoI minimization problems according to the closed-form expressions of AAoI, and give the selection of optimal parameters according to the analysis and simulation. Simulation results verify the accuracy of the theoretical analysis, and show that the AAoI performance of the proposed ACFA protocol is better than that of the FA protocols, and outperforms the REARLY-5 scheme [23] in both dense and sparse access models.

The remainder of the paper is organised as follows. We start our work in Section II by introducing the access model and the AAoI sampling method. To emphasize the freshness of proposed protocol, we first describe the standard frameless ALOHA protocol and our access-banned policy in Section III. We mainly utilize the itereator method to analyze the asymptotic behavior of protocol, and obtain the normalized AAoI formulas in Section IV. The optimal problem and numerical results are given in Section V. Finally, conclusions are drawn in Section VI.

II. System Model

We consider a typical synchronous slot uplink random access scheme [29], where M consecutive slots are organized in medium access control (MAC) frames, and M is the frame length. Moreover, all UEs and the BS are frame and slot synchronous with each other, and a UE schedules at most one packet transmission in each frame, and the channel is modeled as collision channel [29], [30]. Accordingly, the BS receives the superimposed signal from multiple UEs in each slot, and the BS can identify the following three situations according to the received signal power: a) *Silence*, there is no activated UE transmitting in this slot; b) *Singleton*, there is a single UE transmitting replica in this slot, where the slot is called singleton slot; c) *Collision*, multiple UEs transmit replicas in this slot, and a collision occurs. Without loss of generality, when a singleton slot is detected by BS, it will always be successfully decoded if the received signal-to-noise ratio is larger than a predetermined threshold [31]. When a collision is detected, the BS will perform SIC to recover the information in the slot at the end of this frame.

We call the above scheme defined on collision channels a "frame-based" scheme, for the following reasons,

1) For any UE participating in the access, although multiple replicas of data packets can be transmitted in one frame, the valid information transmitted in one frame is always one data packet.
2) In the uplink mMTC scenario, the minimum unit of data transmission is a slot, but the minimum unit of performance parameters analysis is the MAC frame.
3) In a frame, the transmission slots selected by N_t UEs on M slots constitute a $N_t \times M$ transmission matrix, which is related to the corresponding parity check matrix of LDPC code or the LT code. The BS performs the SIC process on this transmission matrix, which is equivalent to performing BP decoding for the LDPC code or the LT code.

Then, we introduce the access model and the sampling method of AoI in detail, which are related to the specific performance analysis of the ACFA random access protocol.

A. Access Model

In order to limit the randomness of UEs and facilitate subsequent discussions, we define two access models as shown

in Fig. 1. The access model in our paper refers to the mode of whether the UEs plans to transmit data packets in one frame. Therefore, here we mainly discuss the relationship between the number of active UEs N_a and the total number of UEs N, and our measure is the average number of active UEs $\mathbb{E}[N_a]$.

1) Dense Access: The most common access model that all potential access UEs are activated on each frame as shown in Fig. 1(b), that is, the activation probability $\pi = 1$ and $\mathbb{E}[N_a] = N_a = N$. Most frame-based protocols use this access model to analysis [7], [8], [32], and we also utilize the dense access model as the starting point of our work.

2) Sparse Access: Contrary to the dense access, we suppose that each UE is activated with a small π at the beginning of the frame as shown in Fig. 1(c). In this case, the average number of activated UEs is $\mathbb{E}[N_a] = \pi N$. The activation probability π in the sparse access model is a key parameter, and we assume that $\pi \leq 0.2$ to ensure the sparsity.

In fact, when π gradually approaches to 1, there is no clear boundary between the two access models, so the above assumptions of π are very necessary, and we keep the $\mathbb{E}[N_a]$ of the two access models at the same order of magnitude to facilitate our discussions.

Similarly, no matter which access model is adopted, we assume that the total number of potential access UEs is N, and each UE in the uplink system has an identification (ID). The details are in Sec. III. Since a UE is assigned an ID, we use subscript i to indicate the UE as U_i.

B. Age of Information and Sampling Method

In order to measure the freshness of information, we denote the current AoI of U_i in the k-th frame as $A_i^{(k)}(t)$, where t is the slot index in the k-th frame. We assume that AoI starts at 0, i.e. $A_i^{(1)}(1) = 0, \forall i \in \{1, 2, \ldots, N\}$, and $A_i^{(k)}(t)$ is incremented by one for each slot in the frame. Since the frame-based protocol only performs SIC at the end of the frame, the current AoI has been increasing steadily within the frame. On the other hand, denote the slot index sampled by U_i in the k-th frame as $T_i^{(k)}$, then the change of the current AoI at the end of the frame can be expressed as:

$$A_i^{(k+1)}(1) := \begin{cases} A_i^{(k)}(M) + 1, & \text{if } U_i \text{ is not recovered at } M, \\ M - T_i^{(k)} + 1, & \text{if } U_i \text{ is recovered at } M. \end{cases} \tag{1}$$

The above formula establishes the AoI connection between frames, so that the AAoI of U_i can be expressed as:

$$\bar{A}_i := \lim_{k \to \infty} \frac{1}{K} \sum_{k=1}^{K} \sum_{t=1}^{M} A_i^{(k)}(t). \tag{2}$$

Note that the AoI increases linearly in steps over time or slots when no update is recovered successfully. We follow this setting and calculate the AoI in frames. Thus, the AAoI of the system can be expressed as:

$$\bar{A} := \frac{1}{N} \sum_{i=1}^{N} \bar{A}_i. \tag{3}$$

In Eq. (1), a key parameter is the slot index when the UE samples, which affects the updating of the AoI of the successfully decoded UEs. Similar to [23], we also define two AoI sampling methods as follows as shown in Fig. 2:

G1: $T_i^{(k)} = 1, \forall i$, each UE performs the sampling process at the beginning of the frame.

GT: $T_i^{(k)} = s_1^i, \forall i$, where s_1^i is the slot number of the first replica of the packet transmitted by U_i. In this case, the UE samples the AoI in real time when transmits the first packet.

III. Age-Critical Frameless ALOHA Protocol

In this section, we mainly describe a simple access protocol from frame-based protocol family, the frameless ALOHA (FA) protocol, and describe our proposed access-banned policy. Finally, the specific access process of the proposed ACFA protocol is given.

A. Standard Frameless ALOHA Protocol

The basic settings of FA protocol are as follows [33]:

- It is a protocol defined based on the MAC frame. For each slot in a frame, the active UE chooses whether to transmit a replica or not with a fixed probability, which is called the access probability. Each replica has one or more pointers pointing to the slot indexes of other replicas transmitted by the same UE.
- The BS can buffer the entire MAC frame, and the BS uses the SIC for decoding after receiving a frame with the help of pointers.

From the above, the FA protocol is a completely distributed, grant-free protocol. In fact, the FA protocol can be seen as a simplified version of the IRSA protocol [34]. In the IRSA protocol, each UE controls the number of replicas transmitted by itself through a degree distribution, which can be represented by a polynomial [30]. In related studies [35], the access probability p is generally indirectly controlled by another parameter β defined as $p = \beta/N_t$, where N_t means the number of accessed UEs, and β removes the influence of the number of accessed UEs. β is conducive to asymptotic analysis and also simplifies the search for optimal parameters. Therefore, in the following, we mainly discuss β rather than p.

Another aspect is the packets recovery rate (PRR) analysis of the FA protocol denoted by p_r, which represents the ratio of the number of UEs successfully decoded after the SIC process in one frame to the number of accessed UEs in one frame. Similarly, we define the normalized system load $g = N_t/M$ in the FA protocol, which is expressed as the ratio of the number of accessed UEs N_t to the frame length M. Further, the throughput of the protocol is denoted as gp_r. At this time, p_r can be seen as a function of N_t, M and β. In the asymptotic regime, that is, $N_t \to \infty$ and $M \to \infty$, p_r can be regarded as a function of g and β. It is shown in [12] that, under this asymptotic regime, the PRR of the FA can be analyzed using an AND-OR tree method [32], by establishing a connection between the SIC process and the decoding of the LT code on the binary erasure channel. Based on the above, p_r can be obtained by a set of iterative formulas.

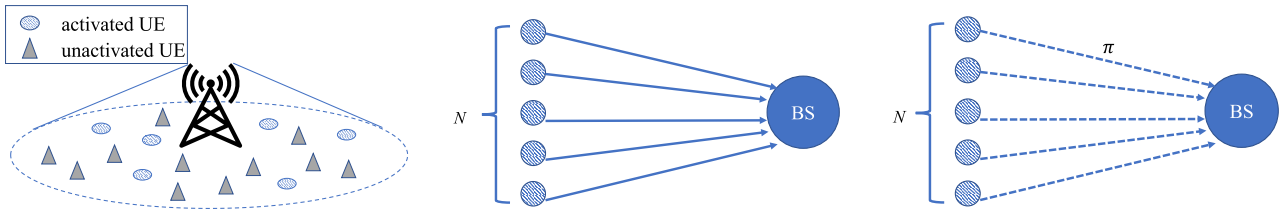

(a) System model. (b) Dense access model. (c) Sparse access model.

Fig. 1. The massive access scenario and two access models. The average number of activated UEs $\mathbb{E}[N_a]$ is N and πN in dense and sparse access models, respectively. The dotted line in (c) indicates that the UEs are activated according to the activation probability π and access to BS.

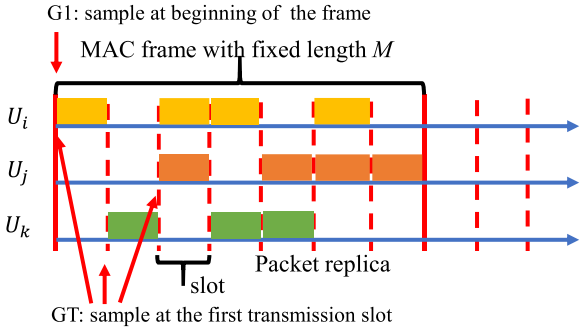

Fig. 2. The AoI sampling method in frame-based protocol.

First, we utilize the generator polynomial form to define the UE node and slot node-respective degree distributions as follows [8], [33],

$$\Lambda(x) = \sum \Lambda_i x^i, \text{and } \mathrm{P}(x) = \sum P_i x^i, \tag{4}$$

where Λ_i represents the probability that a UE node transmits i replicas in a frame, and P_i represents the probability that a slot node has i replicas in a frame, and x is a virtual variable of polynomial. Thus, the edge-respective degree distribution can be expressed as:

$$\lambda(x) = \Lambda'(x)/\Lambda'(1), \text{and } \rho(x) = \mathrm{P}'(x)/\mathrm{P}'(1). \tag{5}$$

For the FA protocol, the probability of each UE accessing on a slot is β/N_t, and there are M slots in one frame, so Λ_i obeys the binomial distribution with parameters M and β/N_t, which can be approximated by a Poisson distribution in the asymptotic regime. It can be expressed as follows:

$$\Lambda_i = \binom{M}{i}(\beta/N_t)^i(1-\beta/N_t)^{M-i} \approx \frac{(\beta/g)^i}{i!}e^{-\beta/g}, \tag{6}$$

where we use $g = N_t/M$ for substitution, which ensures that the above expression is only related to g and β. Thus, $\Lambda(x)$ can be expressed as:

$$\Lambda(x) = \sum \Lambda_i x^i = \sum \frac{(\beta/g)^i}{i!}e^{-\beta/g}x^i = e^{-(\beta/g)(1-x)}, \tag{7}$$

and the corresponding UE node edge-respective degree distribution can be shown as:

$$\lambda(x) = \Lambda'(x)/\Lambda'(1) = e^{-(\beta/g)(1-x)}. \tag{8}$$

Similarly, the slot node edge-respective degree distribution can be obtained as:

$$\rho(x) = \mathrm{P}'(x)/\mathrm{P}'(1) = e^{-\beta(1-x)}. \tag{9}$$

According to Eq. (8) and (9), the iterative expressions of the AND-OR tree analysis of the FA protocol can be expressed as follows:

$$q_j = \lambda(r_{j-1}) = e^{-\beta(1-r_{j-1})/g}, \tag{10}$$

and

$$r_j = 1-\rho(1-q_j) = 1-e^{-\beta q_j}, \tag{11}$$

where q_j and r_j are the average probability that there is an edge connected to the UE and slot nodes during the j-th iteration, respectively. The average probability of UEs recovered after the j-th iteration is expressed as $p_r^{de} = 1-q_j$.

Note that in the above AND-OR tree analysis, p_r^{de} can be regarded as a function of g and β, which can be written as follows:

$$p_r^{de} = f(g,\beta). \tag{12}$$

We will use this form in the derivation in Sec. IV.

B. Access-Banned Policy

We propose the access-banned policy according to our two findings. Specifically,

- In CSA protocol, UE should not perform retransmission operations, and drop the recovery unsuccessfully packets in the frame in order to achieve the minimum AoI [21], [29].
- In the case of limited M slots in mMTC service with a large number of UEs, the UE with low AoI should cancel the transmission plan to provide for the access and update of other UE with high AoI, in order to make the overall AAoI lower [36], [37].

A feasible policy is to give an AoI threshold, if the current AoI of each UE is greater than the threshold, the access is allowed, otherwise the access is banned. This policy has a large gain on slotted ALOHA [28], however the slotted ALOHA protocol is not a frame-based protocol. Thus, we propose the access-banned policy, regard frame as the unit of access as follows:

Access-banned Policy: The UE that successfully decodes in the current frame is banned in the access of the next frame. According to whether access of UE is banned, we divide UEs

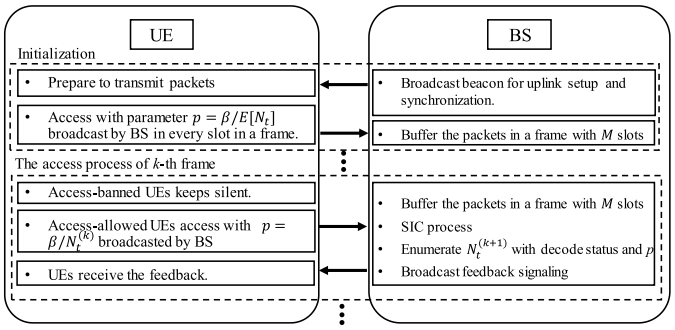

Fig. 3. The access process of proposed ACFA random access protocol.

into two categories: **access-banned** UEs and **access-allowed** UEs.

To support the above policy, recall that our system model has following assumptions:

- UEs in the system have IDs.
- The BS can broadcast the access parameters, and there is a feedback channel to inform the UEs whether the decoding is successful on the current frame.

Based on the above assumptions, our proposed ACFA protocol consists of two parts as shown in Fig. 3:

- The frameless ALOHA protocol.
- Access-banned policy that does not depend on the access model and AoI sampling model.

Moreover, the initialization of our ACFA random access protocol is as follows, the BS first broadcasts the beacon to establish the uplink and perform synchronization. The parameter p is broadcast by the BS through the beacon, and is set to[1] $p = \beta/\mathbb{E}[N_t]$, where β is predefined, and $\mathbb{E}[N_t]$ is the predicted number of access-allowed UEs. The UEs receive the beacon and prepare to transmit their packets in the next frame. Then, the detail procedure of the k-th frame in our ACFA random access protocol is as follows:

Step 1: When the activated UE receives the feedback signal of the $(k-1)$-th frame, if it is allowed to access the BS, it will access with independent probability $p = \beta/N_t^{(k)}$. If UE is not allowed to access, the UE keeps silent in the k-th frame. Note that access-allowed UEs still access according to uncoordinated contention methods, so the ACFA protocol is a grant-free scheme.

Step 2: When the BS receives the whole k-th frame, it performs the SIC process recovering packets. Then, the BS estimates[2] the number of access UEs in the next frame according to the decode status and p, and broadcasts the beacon for synchronization and updated $p = \beta/N_t^{(k+1)}$. The BS broadcasts feedback signal containing the list of access-banned UEs for the next frame.

In the above steps of ACFA random access protocol, we omit the description related to AoI. In fact, AoI is only used as an indicator to measure the performance of the system.

[1]In fact, the initial value of p does not affect the performance of the system after reaching steady state, only the time it takes to reach steady state.

[2]In dense access method, the N_t can be calculated exactly with the $N_t^{(k+1)} = N - N_R^{(k)}$. But it is difficult to estimates the N_t in sparse access, due to the complex relationship between activated UEs and banned-access UEs. The active UEs estimation can be find in [38], [39], and [40].

In our model, it can be implicitly assumed that there is a total of N column caches at the BS, each column corresponds to a potential access UE, and the AoI is obtained by calculating and accumulating the slot difference of the update time-stamp of the UE transmitted. The BS records the AoI in the cache. However, these buffers are not necessarily required in an actual BS.

Note that our proposed access-banned policy can also be extended to all frame-based protocols, such as CRDSA, IRSA, CSA and other protocols. In this paper, we take ACFA protocol as the main analysis object in Sec. V.

IV. ASP and AAoI Performance of ACFA Protocol

In this section, we discuss how to calculate the ASP of ACFA protocol in the asymptotic regime, and derive the close-form expressions of AAoI for ACFA protocol under two access models and two AoI sampling methods, respectively.

A. Parameters and Metrics for ACFA Protocol

Before going into the derivation of ASP, we need to review the parameters and the metrics used in this section. We define η as the ratio of the total activated UEs N to the frame length M as follows,

$$\eta := \frac{N}{M}, \tag{13}$$

and called the virtual code rate of the ACFA protocol, since this ratio is not equal to the actual number of UEs participating in access to the frame length. In the k-th frame, the number of activated UEs, access-allowed UEs, and decoded successfully UEs are $N_a^{(k)}, N_t^{(k)}, N_R^{(k)}$, respectively. Activated UEs is discussed in Sec. II, only relevant to the access model. The access-allowed UEs, who are activated and allowed to access in this frame, are affected by the access model and the access-banned policy, which is also the key to our analysis of the ASP. The number of successfully decoded UEs is related to the SIC decoding itself, and is affected by the parameters N_t, M and β. Therefore, we define the average number of UEs who are activated, access-allowed, and decoded successfully as follows,

$$\mathbb{E}[N_a] = \lim_{K\to\infty} \frac{1}{K} \sum_{k=1}^{K} N_a^{(k)}, \tag{14}$$

and

$$\mathbb{E}[N_t] = \lim_{K\to\infty} \frac{1}{K} \sum_{k=1}^{K} N_t^{(k)}, \tag{15}$$

and

$$\mathbb{E}[N_R] = \lim_{K\to\infty} \frac{1}{K} \sum_{k=1}^{K} N_R^{(k)}, \tag{16}$$

respectively, where the average normalized system load G_a of ACFA protocol is related to $\mathbb{E}[N_t]$ and is defined as:

$$G_a := \frac{\mathbb{E}[N_t]}{M}. \tag{17}$$

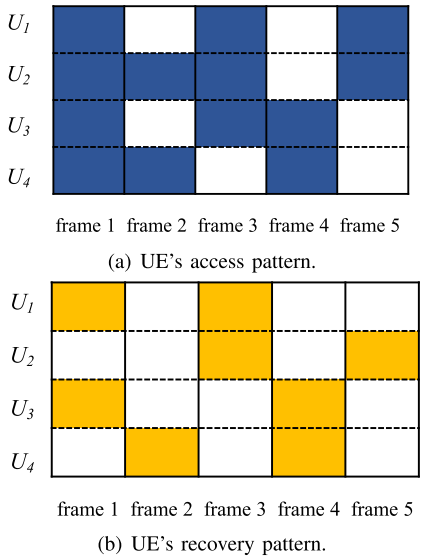

Fig. 4. Example of evolution of N_t and N_R in ACFA protocol with dense access model. Access operation of the UEs is reported in (a), filled rectangles indicate the access-allowed UEs. Recovery operation of the UEs is shown in (b), filled rectangles indicate the UEs with successful recovered packets.

Similarly, the ASP of ACFA protocol P_s is related to $\mathbb{E}[N_R]$ and $\mathbb{E}[N_t]$, and is defined as follows:

$$P_s := \lim_{k\to\infty} \frac{\sum_k N_R^{(k)}}{\sum_k N_t^{(k)}} = \frac{\mathbb{E}[N_R]}{\mathbb{E}[N_t]}. \tag{18}$$

Finally, we discuss these number of UEs with the given example in dense access model, where all the UEs are activated to prepare to access, i.e., $N_a^{(k)} = N, \forall k$. The evolution of N_t and N_R in the ACFA protocol is shown in Fig. 4, with the simple case of $N = 4$ and $M = 5$. Firstly, all UEs are allowed to access the BS in the first frame i.e., $N_t^{(1)} = N$. Then, the packets transmitted by U_1 and U_3 are successfully recovered, thus $N_R^{(1)} = 2$. In frame 2, U_1 and U_3 are banned to transmit packets, and U_2 and U_4 participate in access process, which means $N_t^{(2)} = 2$. Therefore, we get the trend of N_t and N_R in this example, denoted by $\{N_t^{(k)}\} = \{4, 2, 3, 2, 2\}$, $\{N_R^{(k)}\} = \{2, 1, 2, 2, 1\}$. We have

$$N_R^{(k)} \le N_t^{(k)} \le N \quad \forall k = 1, 2, 3, \ldots. \tag{19}$$

B. ASP in ACFA Protocol

One of the contributions of this paper is to derive the iterative expression of the ASP for ACFA protocol, where we give in the following Theorem 1 and Theorem 2.

Theorem 1: The asymptotic ASP of the ACFA protocol in the ***dense access model*** P_s^{de} *can be obtained through the iterative method described by the following two points*:

- *The initial value of the iteration variable x is 1, i.e., $x^{(1)} = 1$;*
- *The iteration variable x using fixed point iteration scheme as follows: $x^{(k+1)} = \phi(x^{(k)})$, where $\phi(x) = 1 - xf(\eta x, \beta)$, and $f(\eta x, \beta)$ is the PRR of the FA protocol obtained by the AND-OR tree analysis mentioned in Sec. III.*

Under the above iterative method, P_R^{de} is expressed as:

$$P_s^{de} = \lim_{k\to\infty} f(\eta x^{(k)}, \beta). \tag{20}$$

Proof: We first consider the evolution of the number of accessed UEs $N_t^{(k)}$, which is the key and difficulty to analyze the asymptotic ASP in our ACFA protocol. Note that we use $\tilde{\circ}$ to describe the normalized number of UEs, where $\tilde{N}_a^{(k)} = N_a^{(k)}/N$, $\tilde{N}_t^{(k)} = N_t^{(k)}/N$, and $\tilde{N}_R^{(k)} = N_R^{(k)}/N$. Thus, we can observe from Fig. 4 that in the k-th frame, there are $N_R^{(k)}$ UEs decoded successfully and in the $(k+1)$-th frame there are $N_a^{(k+1)}$ UEs activated and $N_t^{(k+1)}$ UEs access-allowed, and we have,

$$N_t^{(k+1)} + N_R^{(k)} = N_a^{(k+1)}. \tag{21}$$

In the dense access model, the number of activated UEs is always equal to the number of total UEs in the system, which means $N_a^{(k)} = N, \forall k$. Thus, we can obtained the normalized number of UEs as follows,

$$\tilde{N}_t^{(k+1)} + \tilde{N}_R^{(k)} = 1. \tag{22}$$

Here we can estimate the $\tilde{N}_R^{(k)}$ with p_r^{de} and $\tilde{N}_t^{(k)}$ in the asymptotic regime as follows,

$$\begin{aligned}\tilde{N}_R^{(k)} &= \tilde{N}_t^{(k)} f(N_t^{(k)}/M, \beta) \\ &= \tilde{N}_t^{(k)} f(\tilde{N}_t^{(k)} \frac{N}{M}, \beta) = \tilde{N}_t^{(k)} f(\eta \tilde{N}_t^{(k)}, \beta).\end{aligned} \tag{23}$$

By substituting into Eq. (22), we have

$$\tilde{N}_t^{(k+1)} = 1 - \tilde{N}_t^{(k)} f(\eta \tilde{N}_t^{(k)}, \beta). \tag{24}$$

Let $\phi(x) = 1 - xf(\eta x, \beta)$, and the $\tilde{N}_t$ is the iteration variable. Now, we have established the relationship between the number of access-allowed UEs from frame to frame, using the fixed point iteration method described above. One question is that whether $\tilde{N}_t$ converge to a fixed point in this iterative method. In this regard, we first analyze $\phi(x)$. The most critical part of this function is the PRR of FA protocol $f(\eta x, \beta)$, but this function does not have an analytical expression, so we can only take some specific parameters η and β for rough verification.

Fig. 5 shows the PRR curves for some specific η and β. For the fixed point iteration method, the iterative process is represented as follows and shown in Fig. 5(b) and 5(c).

Step 0: Find the point $(1, \phi(1))$ as the starting point of the iteration method on the graph. At this time $x^{(2)} = \phi(1)$.

Step 1: Make a vertical line to the y-axis and the line $y = x$ compared to the point p_1. The coordinates of the point are $(\phi(\phi(1)), \phi(1))$, and $x^{(3)}$ is the value of x-axis.

Step 2: Make a vertical line to the x-axis at point p_1, and intersect the curve $y = \phi(x)$ at the point p_2, and $x^{(3)}$ is the value of y-axis.

Step 3: Repeat **Step 1** and **Step 2**, and finally $x^{(k)}$ converges to the first intersection of the curve $y = \phi(x)$ and the straight line $y = x$ from right to left.

To finish the proof, we first need to ensure that there is at least one intersection point between the line and the curve.

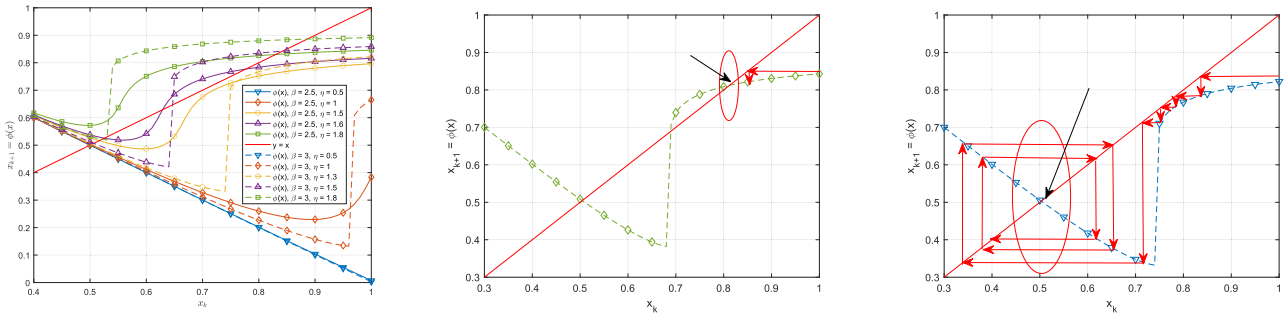

(a) The iterative function $\phi(x)$ under different η (b) The iterative process of $\phi(x)$, $\beta = 3$, $\eta = 1.4$. (c) The iterative process of $\phi(x)$, $\beta = 3$, $\eta = 1.3$ and β.

Fig. 5. The iterative method. The iteration starts from point (1,$\phi(1)$), and converges to the intersection of $y = \phi(x)$ and $y = x$ closet to the start point.

In this regard, we let $\mathcal{L}(x) = \phi(x) - x$, then the function $\mathcal{L}(x)$ is continuous on $[0, 1]$, and it is easy to know:

$$\mathcal{L}(0) = 1, \mathcal{L}(1) = -f(\eta, \beta) < 0,$$

Therefore, there is $\mathcal{L}(0) \cdot \mathcal{L}(1) < 0$, i.e., $\mathcal{L}(x)$ must have zero point on $[0, 1]$, so the line and the curve has at least one intersection.

Now we have proved that under this iterative method, the system will eventually be in a stable state. We use $\circ^*$ to mark various parameters in this stable state, such as the number of UEs access-allowed in a frame is N_t^*, and each frame is successfully decoded with N_R^* UEs. According to Eq. (18), the ASP in steady state can be expressed as:

$$\begin{aligned} P_s^{de} &= \frac{N_R^*}{N_t^*} = \frac{\tilde{N}_R^*}{\tilde{N}_t^*} = \frac{\tilde{N}_t^* f(\eta \tilde{N}_t^*, \beta)}{\tilde{N}_t^*} \\ &= f(\eta \tilde{N}_t^*, \beta) = \lim_{k \to \infty} f(\eta \tilde{N}_t^{(k)}, \beta), \text{ with } \tilde{N}_t^{(1)} = 1, \end{aligned} \tag{25}$$

which completes the proof. ■

In the above proof, when the system is in steady state, we can also measure the normalized system load of the system as:

$$G_a = \frac{\mathbb{E}[N_t]}{M} = \frac{N_t^*}{M} = \eta \tilde{N}_t^*. \tag{26}$$

In fact, we can only specify the virtual code rate η of the system, and cannot know the overall normalize system load G_a, we can still use the above iterative method to analyze G_a.

In order to verify the accuracy of asymptotic ASP via the iterative method, we carry out simulations including ASP, G_a, and throughput under three sets of parameters as shown in Fig. 6, the detailed parameters are: $N = [100, 500, 1000]$, $\beta = 3$, η in the range of $[1, 2]$ with a step of 0.05, and the corresponding $M = \lfloor N/\eta \rfloor$.

Fig. 6(a) shows the ASP versus the virtual rate η, Fig. 6(b) shows the normalized system load G_a versus η and Fig. 6(c) shows the corresponding throughput performance of our ACFA protocol, we can obtain the suitable η from the simulation results. We first obtain the number of access-allowed UEs in the steady state $\tilde{N}_t^*$ via the iterative method. Then, the corresponding ASP is obtained by $f(\eta \tilde{N}_t^*, \beta)$, the corresponding G_a curve is obtained by $\eta \tilde{N}_t^*$, and the throughput under the corresponding η is obtained by multiplying G_a with ASP.

Furthermore, the simulated ASP in Fig. 6(a) gradually approaches the asymptotic theoretical curve with the increasing of N, and when $N = 500$, it can agree well with the asymptotic curve. Similarly, the asymptotic throughput can also agree well with the simulation point when $N = 500$, and achieves 0.74. For the asymptotic theoretical curve, there is a jump point at $\eta \approx 1.34$, and the ASP curve jumps from close to 0.98 to around 0.29. We denote η corresponding to this jump point as η_τ, and divide the entire curve into three regions: 1) $\{\eta < \eta_\tau, P_s \approx 1\}$, there is almost no performance degradation; 2) $\{\eta > \eta_\tau, P_s < 0.3\}$, these above two regions are called linear regions. 3) The last region is $\{\eta \approx \eta_\tau\}$, named the jump region, and pay more attentions to the left of the jump point, marked as η_τ^-. At the point η_τ^-, ASP is still at the a higher level, and the corresponding η is the largest. Similarly, for the simulation points, we also observed this jump phenomenon, and when $N = 500, 1000$, both jumping occur around $\eta = 1.40$. Note that Fig. 6(b) and 6(c) also have this jump phenomenon.

A fundamental cause of the jump phenomenon is the $\phi(x)$ function as shown in Fig. 5, which is determined by the PRR of FA protocol p_r. It can be observed from the two curves with $\eta = 1.3, 1.5$, $\exists \eta_\tau \in [1.3, 1.4]$, the curve $y = \phi(x)$ and the line $y = x$ have a tangent point at about $x = 0.8$, which makes the convergence point jump from $x \approx 0.5$ to $x \approx 0.8$ in the iteration method, causing the jumping phenomenon in Fig. 6. In a physical sense, the decoding result of the previous frame determines the decoding result of the next frame due to the access-banned policy, i.e., they are coupled, which leads to a consistent decoding rate of two adjacent frames. Thus, the system performance varies rapidly after η exceeds a threshold in the FA protocol.

Then, we discuss the asymptotic ASP in the sparse access model. We also utilize the above fixed point iteration method and give the following Theorem 2:

Theorem 2: The asymptotic ASP of the ACFA protocol in the ***sparse access model*** P_s^{de} *can be obtained through the iterative method described by the following two points*:

- *The initial value of the iteration variable x is π, i.e., $x^{(1)} = \pi$;*

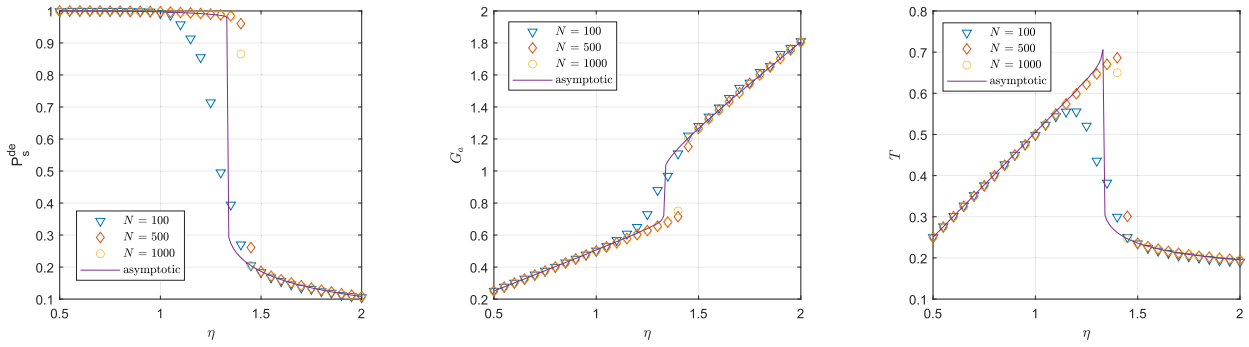

(a) ASP v.s. η (b) G_a v.s. η (c) Throughput v.s. η

Fig. 6. The result of simulation and asymptotic curve using iterative method for ASP performance, system load estimation, and throughput performance of ACFA protocol in dense access model.

- *The iteration variable x using fixed point iteration method as follows: $x^{(k+1)} = \psi(x^{(k)})$, where $\psi(x) = \pi(1 - xf(\eta x, \beta))$, and $f(\eta x, \beta)$ is also the PRR of the FA protocol obtained by the AND-OR tree analysis mentioned in Sec. III.*

Under the above iterative method, P_s^{de} is expressed as:

$$P_s^{de} = \lim_{k\to\infty} f(\eta x^{(k)}, \beta). \tag{27}$$

Proof: We start from the number of access-allowed UEs in the $(k+1)$-th frame $N_t^{(k+1)}$, and the remaining number of UEs who are activated but banned to access, denoted as $N_{a,b}^{(k+1)}$, together constitute the total number of activated UEs in the $(k+1)$-th frame $N_a^{(k+1)}$, as follows:

$$N_a^{(k+1)} = N_{a,b}^{(k+1)} + N_t^{(k+1)}, \tag{28}$$

where $N_{a,b}^{(k+1)}$ can be expressed as the product of the total number of UEs, the activation probability π and the probability of banned, i.e., $N \cdot \pi \cdot p_b$. Because the access-banned UEs are successfully decoded in the k-th frame, so p_b can be expressed as the probability of successful decoding in the k-th frame with $p_b = N_R^{(k)}/N = \tilde{N}_R^{(k)}$. The expectation of the above expression can be expressed as:

$$\pi N = \mathbb{E}[N_t^{(k+1)}] + \mathbb{E}[N\pi\tilde{N}_R^{(k)}] = \mathbb{E}[N_t^{(k+1)}] + \pi N\mathbb{E}[\tilde{N}_R^{(k)}]. \tag{29}$$

Arranging this expression, the normalized number of access-allowed UEs in the $(k+1)$-th frame can be expressed as:

$$\mathbb{E}[\tilde{N}_t^{(k+1)}] = \pi(1 - \mathbb{E}[\tilde{N}_R^{(k)}]). \tag{30}$$

We can also use the PRR of FA to estimate the number of UEs decoding successfully in the k-th frames, then an approximate iterative method of the above expression can be expressed as:

$$\tilde{N}_t^{(k+1)} = \pi(1 - \tilde{N}_t^{(k)} f(\eta\tilde{N}_t^{(k)}, \beta)). \tag{31}$$

We follow the process used in Theorem 1 and let $\psi(x) = \pi(1 - xf(\eta x, \beta))$, then $\tilde{N}_t$ is the iteration variable. Similarly, this iterative method will eventually reach a stable state. The proof is similar to Theorem 1. We also denote $\tilde{N}_t$ when the system reaches a steady state as $\tilde{N}_t^*$, and the asymptotic ASP can also be obtained as:

$$P_s^{de} = f(\eta\tilde{N}_t^*, \beta) = \lim_{k\to\infty} f(\eta\tilde{N}_t^{(k)}, \beta), \text{ with } \tilde{N}_t^{(1)} = \pi, \tag{32}$$

which completes the proof. ■

Note that in the sparse access model, the ratio of N to M is usually fixed, and the number of UEs activated in a frame is adjusted by the activation probability π. Similar to the virtual code rate η in the dense access model, we need to define a virtual code rate ζ to characterize the activated UEs load, which is defined as the ratio of the average number of activated UEs to the frame length as $\zeta = \mathbb{E}[N_a]/M$. Recall that in the dense access model, we use η as this indicator, because of $\mathbb{E}[N_a] = N$ and $\zeta = \mathbb{E}[N_a]/M = N/M = \eta$. In the sparse access model, we have,

$$\zeta = \frac{\mathbb{E}[N_a]}{M} = \frac{\pi N}{M} = \pi\eta, \tag{33}$$

where $\zeta < 1$ indicates that the number of activated UEs is less than the frame length, but ζ cannot be used as a basis for judging whether the system is overloaded, because $N_a \neq N_t$.

Similarly, in order to verify the accuracy of asymptotic ASP, we simulated the ASP, G_a and throughput versus different ζ, and the parameters are $N = [10^3, 5\times10^3, 10^4]$, $\eta = 10, \beta = 3$, $M = N/\eta$, π in the range of $[0.5, 2]$. We also use the iterative method to get the asymptotic performance and draw in Fig. 7, marked with a solid line.

With the same growth of N and M, the simulation point is getting closer to the asymptotic curve. Note that the ASP in Fig. 7(a) in the sparse access model still has jumps, which is related to the parameter η. When the relevance of UEs are weakened, the number of banned UEs is reduced. In this case our access-banned policy will gradually fail, but there are still some performance gains.

Unlike the dense access model, the number of access-banned UEs is significantly reduced, making G_a versus ζ in Fig. 7(b) almost close to the line $y = x$ without obvious discontinuities. Note that the analysis in asymptotic regime is still valid, and we can select the suitable ζ from the simulation results. Fig. 7(c) shows the throughput performance of the ACFA protocol under the sparse access model, achieving a maximum of 0.85 around $\zeta \approx 1$ in the asymptotic regime. When $N = 100, 500$, the maximum throughput

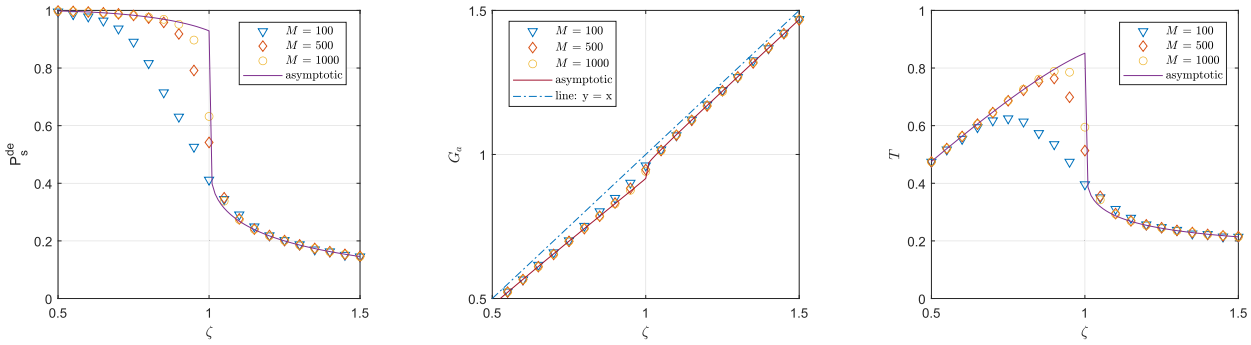

(a) ASP v.s. ζ (b) G_a v.s. ζ (c) Throughput v.s. ζ

Fig. 7. The result of simulation and asymptotic curve using iterative method for ASP performance, system load estimation, and throughput performance of ACFA protocol in sparse access model. The jump phenomenon seems to be improved.

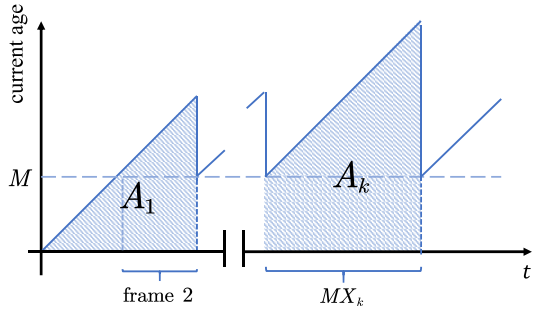

Fig. 8. Example timeline of current age of U_i. Between two recovery process, the number of frame is described as X_k, and the accumulated age is illustrated by shaded area and marked by A_k.

of $0.625, 0.763$ is obtained at $\zeta = 0.75, 0.9$, respectively. In general, its throughput performance is slightly better than that of dense access model. On one hand, fixing M makes the overall code length longer, and on the other hand, $\beta = 3$ is more suitable for sparse access model.

C. AAoI Analysis

In this subsection, we derive the closed-form AAoI expression for the proposed ACFA protocol with the following four Theorems.

Theorem 3: The AAoI of ACFA protocol in dense access model with $G1$ sampling method $\bar{A}_{d,G1}$ is given by

$$\bar{A}_{d,G1} = \frac{3M}{2} + \frac{M}{P_s} - \frac{M}{P_s+1} + \frac{1}{2}, \tag{34}$$

where P_s is the ASP defined in Eq. (18). We can also get the expression of $\tilde{A}_{d,G1}$ after normalized the total number of UEs N,

$$\tilde{A}_{d,G1} = \frac{\bar{A}}{N} \approx \frac{1}{\eta}\left(\frac{3}{2} + \frac{1}{P_s} - \frac{1}{P_s+1}\right). \tag{35}$$

Proof: Consider the current AoI evolution of U_i as shown in Fig. 8. Let $X_k \in \{2, 3, \dots\}$ denote the number of frames between the $(k-1)$-th and the k-th successful packet recovery. Thus, there are MX_k slots between these two recovery process. Hence X_k satisfies $\Pr\{X = k\} = (1-P_s)^{k-2}P_s, k = 2, 3, \dots$, because there are at least two frames between two recovery process. Moreover, when P_s is dependent on β and the SIC process in ACFA protocol and independent on k. Therefore, we derive the first and second moments of X_k as follows,

$$\mathbb{E}[X_k] = \sum_{k=2}^{\infty} k(1-P_s)^{k-2}P_s = \frac{1+P_s}{P_s}, \tag{36}$$

$$\mathbb{E}[X_k^2] = \sum_{k=2}^{\infty} k^2(1-P_s)^{k-2}P_s = \frac{P_s^2+P_s+2}{P_s^2}. \tag{37}$$

Between the $(k-1)$-th and the k-th frame recovery, the accumulated AoI is expressed as A_k, where the AoI starts from M and increases linearly up to $M + MX_k$ except for $k = 1$, marked by shaded area in Fig. 8, and we have

$$A_k = M^2X_k + MX_k(MX_k+1)/2, \tag{38}$$

and the sequence $\{A_k\}$ consists of $i.i.d$ random variables. The AAoI in U_i can be calculated by

$$\begin{aligned}\bar{A}_i &= \lim_{k\to\infty} \frac{\sum_k A_k}{\sum_k MX_k} = \frac{\mathbb{E}[A_k]}{M\mathbb{E}[X_k]} \\ &= M + \frac{M\mathbb{E}[X_k^2]}{2\mathbb{E}[X_k]} + \frac{1}{2} \\ &= \frac{3M}{2} + \frac{M}{P_s} - \frac{M}{P_s+1} + \frac{1}{2}.\end{aligned}$$

Recalling that all UEs access independently, it means $\bar{A}_{d,G1} = \bar{A}_i$ with Eq. (3), which completes the proof. ■

Theorem 4: The AAoI of ACFA protocol in dense access model with GT sampling method $\bar{A}_{d,GT}$ is given by

$$\bar{A}_{d,GT} = \frac{3M}{2} + \frac{M}{P_s} - \frac{M}{P_s+1} + \frac{1}{2} - \mathbb{E}[T], \tag{39}$$

where the average number of indexes of the sampling slot is $\mathbb{E}[T] = \mathbb{E}[N_t]/\beta$, which also is the gain obtained by sampling in the first transmission slot under the GT method. We can also get the expression of $\tilde{A}_{d,GT}$ after normalized N,

$$\tilde{A}_{d,GT} = \frac{\bar{A}}{N} \approx \frac{1}{\eta}\left(\frac{3}{2} + \frac{1}{P_s} - \frac{1}{P_s+1} - \frac{G_a}{\beta}\right). \tag{40}$$

Proof: The proof is similar to the Theorem 3, and the sampling method only affects the calculation of the accumulated AoI A_k. Specifically, for U_i between the k-th and

$(k+1)$-th frames, its AoI starts from $M-T_i$ and increases linearly to $(M-T_i+MX_k)$, and A_k can be expressed as:

$$\begin{aligned} A_k &= \sum_{j=1}^{MX_k} M - T_i + j \\ &= \frac{M^2X_k^2}{2} + \left(M - T_i + \frac{1}{2}\right) MX_k. \end{aligned} \tag{41}$$

Therefore, the AAoI in GT can be expressed as follows:

$$\begin{aligned} \bar{A}_{d,GT} &= \lim_{k\to\infty} \frac{\sum_k A_k}{\sum_k MX_k} = \frac{\mathbb{E}[A_k]}{M\mathbb{E}[X_k]} \\ &= \frac{M\mathbb{E}[X_k^2]}{2\mathbb{E}[X_k]} + M + \frac{1}{2} - \mathbb{E}[T] \\ &= \frac{3M}{2} + \frac{M}{P_s} - \frac{M}{P_s+1} + \frac{1}{2} - \mathbb{E}[T] \\ &= \bar{A}_{d,G1} - \mathbb{E}[T], \end{aligned} \tag{42}$$

Thus, we need calculate $\mathbb{E}[T]$ for all access-allowed UEs. The access-allowed UEs choose whether to transmit replicas with probability p in the M slots, then the index of the first transmission slot follows the geometric distribution, which satisfies $\Pr\{T = s_1\} = (1-p)^{s_1-1}p, s_1 = 1,2,3,\ldots,M$. Thus, $\mathbb{E}[T]$ can be expressed as:

$$\mathbb{E}[T] = \frac{1}{p} = \frac{\mathbb{E}[N_t]}{\beta}, \tag{43}$$

which completes the proof. ■

The above Theorem 3 and Theorem 4 describe the AAoI expression of the ACFA protocol under the dense access model. Among them, GT has one more gain term brought by sampling just in time than $G1$, which is related to the access probability. Since the access probability changes according to the access-banned policy in each frame in the ACFA protocol, we can use the number of access-allowed UEs in the steady state N_t^* to calculate the probability.

Fig. 9(a) shows the AAoI performance in the above two sampling methods. We simulate with $N = 100, 500$, $\beta = 3$. When $N = 500$, the simulated $\tilde{A}_d$ basically fit $\tilde{A}_d^{de}$, and at $\eta \approx 1.35, 1.40$, the ACFA protocol reaches the minimum AAoI $\tilde{A}_{d,G1} = 1.493$ for $G1$ and $\tilde{A}_{d,GT} = 1.312$ for GT, with $M = \lfloor 500/1.4 \rfloor \approx 357$. We have analyzed the jump phenomenon at Fig. 6(b), which can also be used to explain the jump phenomenon at $\eta = 1.4$. Corresponding to the above, we denote the point where the jump occurs as η_τ, and it is the point with minimum AAoI. For $\eta < \eta_\tau$, all simulation points are very close to the theoretical curve, and there is only a deviation due to the short frame length near this point. When $\eta > \eta_\tau$, there is almost no error in the $G1$ case, and the gain brought by the GT case is not as much as the theoretical analysis.

Next, we will give the AAoI expression under sparse access model.

Theorem 5: The AAoI of ACFA protocol in sparse access model with $G1$ sampling method $\bar{A}_{s,G1}$ is given by

$$\bar{A}_{s,G1} = \frac{M}{2} + \frac{M}{\pi P_s} + \frac{1}{2}, \tag{44}$$

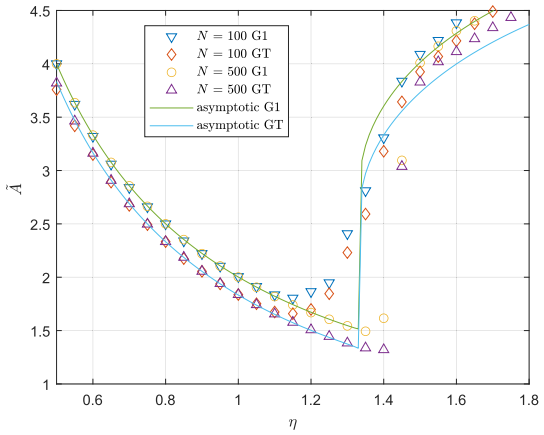

(a) AAoI performance in dense access

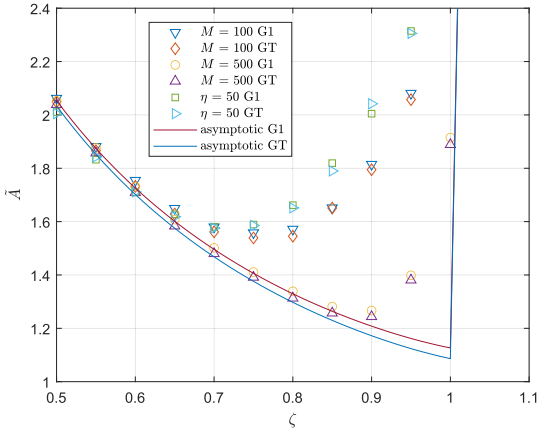

(b) AAoI performance in sparse access.

Fig. 9. AAoI performance of the ACFA protocol in two sampling method with $N = 100, 500$ and $\beta = 3$ versus virtual rate η and ζ in two access models.

and we can also get the normalized AAoI $\tilde{A}_{s,G1}$ as

$$\tilde{A}_{s,G1} \approx \frac{1}{\eta}\left(\frac{1}{2} + \frac{1}{\pi P_s}\right). \tag{45}$$

Proof: We also examine the behavior of X_k, let $p = \pi P_s$ represent the average decoding rate within a frame, as follows:

$$\begin{aligned} &p\{X = k\} \\ &= \begin{cases} P_s, & k = 1, \\ p(1-P_s)^{k-2}P_s + (1-p)(1-P_s)^{k-1}P_s, & k \geq 2, \end{cases} \end{aligned} \tag{46}$$

where X_k consists of two items when $k \geq 2$. When η is large, it means that UEs activation is relatively sparse, and there are very few UEs who are banned for access. We can consider that X_k approximately follows the geometric distribution, satisfying $\Pr\{X = k\} = (1-p)^{k-1}p, k = 1, 2, \ldots$. We also use Eq. (38) to calculate A_k, and the first and second moments of X_k can be expressed as $\mathbb{E}[X_k] = 1/p$ and $\mathbb{E}[X_k^2] = (2-p)/p^2$. Thus, we obtain the above expression and complete the proof. ■

Fortunately, the relationship between $G1$ and GT is also applicable under the sparse access model. Therefore, we give the AAoI expression under GT sampling in the following

Theorem 6, and the proof is similar to the Theorem 4 and Theorem 5, and we omit the proof.

Theorem 6: The AAoI of ACFA protocol in sparse access model with GT sampling method $\bar{A}_{s,GT}$ is given by

$$\begin{aligned}\bar{A}_{s,GT} &= \bar{A}_{s,G1} - \mathbb{E}[T], \\ &= \frac{M}{2} + \frac{M}{\pi P_s} + \frac{1}{2} - \frac{\mathbb{E}[N_t]}{\beta}.\end{aligned} \tag{47}$$

and we can get the normalized AAoI $\tilde{A}_{s,GT}$ as

$$\tilde{A}_{s,GT} \approx \frac{1}{\eta}\left(\frac{1}{2} + \frac{1}{\pi P_s} - \frac{G_a}{\beta}\right). \tag{48}$$

Fig. 9(b) shows the AAoI performance of the ACFA protocol in two sampling methods in sparse access model. Now the key parameter is η, which describes the sparsity of the access process. The larger η is, the sparser the of active UEs in each frame. Therefore, the simulation is divided into three groups, the total number of UEs is $N = [1000, 5000, 5000]$, and the corresponding frame length is $M = [100, 500, 100]$. Then, η of the first two groups is guaranteed in 10. The second and third groups ensure that the total number of UEs is the same, and the impact of the difference in η on the ACFA protocol is verified. In the sparse access model, ζ is mainly used to measure the system load.

It can be seen that the sampling method does not have much influence on the normalized AAoI of the system, so we mainly discuss the comparison between the above three groups. The AAoI performance of the ACFA protocol under the three sets of parameters is convex, and it is a unimodal function about ζ. When the total number of UEs expands, the AAoI of the protocol will tend to the asymptotic curve. Specifically, when N increases from 1000 to 5000, the corresponding lowest normalized AAoI in G1 mode decreases from 1.56 to 1.27, and the corresponding lowest point also shifts from $\zeta = 0.75$ to 0.9. We also found that when the sparsity η increases, the overall AAoI will increase. In general, the ACFA protocol also has a certain performance improvement in the sparse access model, but the gain brought by the access-banned policy will gradually fail with the increasing of the sparseness.

V. Minimum AAoI for ACFA Protocol

In this section, we mainly discuss the choice of parameters β for different N to minimize the AAoI of proposed ACFA protocol, so as to improve the freshness of information. Specifically, we divide it into two parts according to the access model and propose the corresponding optimization problem, and focus on choice of the parameter β in asymptotic regime.

A. Minimum Normalized AAoI in Dense Access Model

Regardless of the access model, in the asymptotic regime, $N \to \infty$, $M \to \infty$, and AAoI $\bar{A} \to \infty$, so we mainly discuss the normalized AAoI. Taking the $G1$ sampling method as an example, under the dense access model, the normalized AAoI optimization problem in the asymptotic regime can be described as follows,

$$\underset{\beta,\eta}{\text{minimize}}\ \frac{1}{\eta}\left(\frac{3}{2} + \frac{1}{P_s^{de}} - \frac{1}{P_s^{de}+1}\right), \tag{49}$$

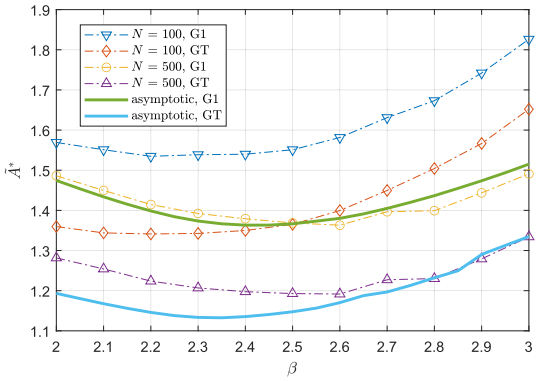

Fig. 10. Minimum normalized AAoI $\tilde{A}^*_{d,G1}$ and $\tilde{A}^*_{d,GT}$ versus β in asymptotic regime and finite length.

which is obtained by substituting P_s^{de} for P_s, and we denote the solution of the problem as $\tilde{A}^*_{d,G1}$.

Similarly, for GT sampling method, there is a normalized AAoI optimization problem as follows,

$$\underset{\beta,\eta}{\text{minimize}}\ \frac{1}{\eta}\left(\frac{3}{2} + \frac{1}{P_s^{de}} - \frac{1}{P_s^{de}+1} - \frac{G_a}{\beta}\right). \tag{50}$$

The above two problems only differ by one item $\frac{G_a}{\beta}$, and there are only two variables to be optimized, so we use a simple traversal method for optimization in the asymptotic regime. We fix β, and use the iterative method proposed by Theorem 1 and Eq. (34) to find the $\tilde{A}^*_{d,G1}$ under this β and the corresponding η. We show the minimum normalized AAoI that can be achieved with different β in Fig. 10. Similarly, we also simulated β versus $\tilde{A}^*_{d,G1}$ under the finite length of $N = 100, 500$, where the step size $\Delta\beta = 0.1$.

Fig. 10 shows the minimum normalized AAoI under different β. $\tilde{A}^*_{d,G1}$ and $\tilde{A}^*_{d,GT}$ are convex functions of β, and they are not sensitive to the change of β near the minimum value. Therefore, the requirement for the accuracy of active UEs detection is low, and a part of the computational overhead can be balanced. The minimum $\tilde{A}^*_{d,G1}$ is obtained around $\beta = 2.5$, and the minimum $\tilde{A}^*_{d,GT}$ is obtained around $\beta = 2.3$ in the asymptotic regime. At $N = 100$, β in the range of $[2, 2.5]$, $\tilde{A}^*_{d,G1}$ and $\tilde{A}^*_{d,GT}$ have a little changes, and get 1.53 and 1.34 respectively. At $N = 500$, the curve in $G1$ sampling method is close to the asymptotic curve, while the GT sampling method has a deviation of about 5% to the asymptotic curve.

According to the approximate optimal β^* obtained in Fig. 10, the AAoI performance of the optimized ACFA protocol compared to the FA protocol as shown in Fig. 11. We note that the optimal β^* of two protocols are different. For the ACFA protocol, the minimum normalized AAoI is almost always obtained near the jump point η_τ, and the corresponding G_a^* is smaller compared to FA protocol. The curve in $N = 500$ is already very close to the asymptotic curve. At $N = 100, 500$, the $\tilde{A}^*_{d,G1}$ of the ACFA protocol reaches $1.54, 1.36$, which is lower than the $2.01, 1.87$ of the FA protocol by $23\%, 27\%$, respectively, as shown in Fig. 11(a). Fig. 11(b) shows that in GT sampling method. At $N =$

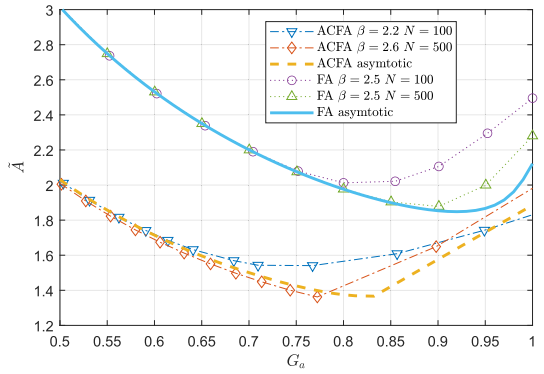

(a) $G1$ sampling method

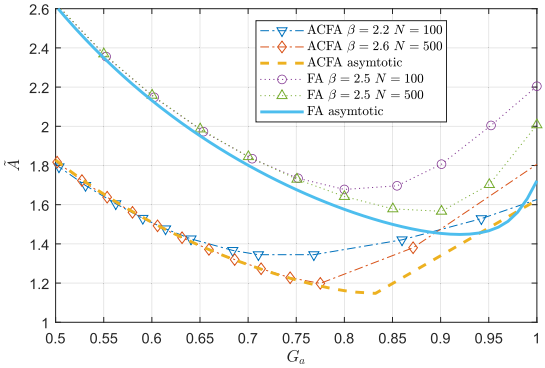

(b) GT sampling method

Fig. 11. The minimum $\tilde{A}_{d,G1}$ and $\tilde{A}_{d,GT}$ versus average system load G_a for frameless ALOHA and ACFA protocol with their own β^* in dense access model.

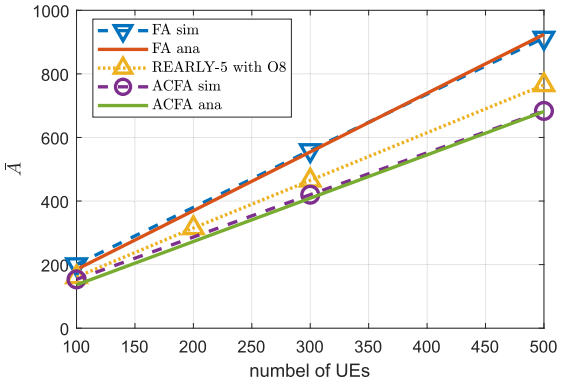

(a) $G1$ sampling method

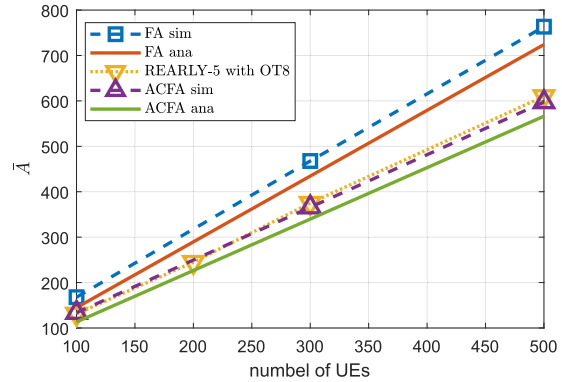

(b) GT sampling method

Fig. 12. $\bar{A}^*$ versus number of UEs N for FA protocol, REARLY-5 scheme and ACFA protocol.

$100, 500$, the $\tilde{A}^*_{d,GT}$ of the ACFA protocol reaches $1.34, 1.18$, which is lower than the $1.68, 1.57$ of the FA protocol by 25% and 33%, respectively. For the ACFA protocol, the gain term in GT is $\frac{G_a}{\beta\eta} = \frac{0.77}{2.6\times1.55} = 0.191$ at $N = 500$, which is consistent with the simulation results. For the FA protocol, since $G_a = \eta$, its gain term is always $1/\beta$, which makes the difference between $\tilde{A}^*_{d,G1}$ and $\tilde{A}^*_{d,GT}$ smaller compared with ACFA protocol.

We finally compare with the corresponding FA and the IRSA-based REARLY-5 schemes in Fig. 12, where the REARLY-5 scheme performs 5 rounds SIC after the end of each slot in the frame. The ACFA protocol is close to the result of the asymptotic analysis when the number of UEs is large in $G1$ sampling method, while there is approximately 7% away from the asymptotic value in GT. In $G1$ sampling method, REARLY-5 uses the optimal degree distribution $O8$ [23], and finally $\tilde{A}^*_{d,G1}$ reaches 1.53. The minimum normalized AAoI for the ACFA protocol reaches 1.36, which is 12.5% lower than REARLY-5. In GT sampling method, the $\tilde{A}^*_{d,GT}$ of the ACFA protocol reaches 1.19, which is slightly lower than 1.22 achieved by REARLY-5 using the optimal degree distribution $OT8$. Overall, ACFA protocol achieves a lower normalized AAoI than the REARLY-5 scheme. We note that REARLY-5 scheme obtains a timeliness gain by decoding each slot early, which increases the computation and complexity, while the ACFA protocol controls access adaptively through the access-banned policy, which only increases the cost of feedback.

B. Minimum Normalized AAoI in Sparse Access Model

In the case of sparse access, η is an uncontrollable variable used to describe the access behavior, so the optimization problem under $G1$ can be written as follows,

$$\underset{\beta,\pi}{\text{minimize}}\ \frac{1}{\eta}\left(\frac{1}{2}+\frac{1}{\pi P_s^{de}}\right), s.t.\ \text{fixed}\ \eta, \tag{51}$$

where P_s^{de} is the ASP in the asymptotic regime, and the solution is denoted as $\tilde{A}^*_{s,G1}$. Similarly, the normalized AAoI optimization problem under GT can be formulated as follows,

$$\underset{\beta,\pi}{\text{minimize}}\ \frac{1}{\eta}\left(\frac{1}{2}+\frac{1}{\pi P_s^{de}}-\frac{G_a}{\beta}\right), s.t.\ \text{fixed}\ \eta. \tag{52}$$

The difference between the above two problems is still $\frac{G_a}{\beta\eta}$, but in the sparse access model, the magnitude of η is larger, making the gain of GT smaller.

For the two sampling methods under sparse access model, we take $\eta = 10, 50$ as an example, obtain the curves about β, $\tilde{A}^*_{s,G1}$ and $\tilde{A}^*_{s,GT}$ with the iterative method in Theorem 2 and Eq. (51-52) as shown in Fig. 13. In the asymptotic regime, $\beta^* \approx 3$, which is consistent with the growth direction of β^* when M increases. Specifically, at $M = 100, 500$, β^* is close to 2.5 and 2.8, respectively. In addition, the two curves of $\eta = 50$ have almost no difference, because the GT gain term is $\frac{0.75}{2.5\times50} = 0.006$. At this time, due to the increasing of η, the lowest $\tilde{A}^*_{s,GT}$ increased from 1.41 to 1.46, and the lowest $\tilde{A}^*_{s,G1}$ from 1.44 to 1.47.

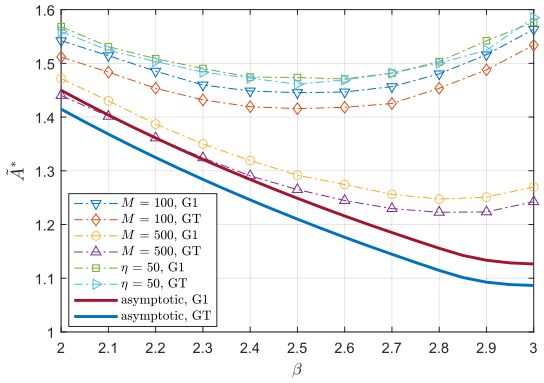

Fig. 13. Minimum normalized AAoI $\tilde{A}^*_{s,G1}$ and $\tilde{A}^*_{s,GT}$ versus β in asymptotic regime and finite length.

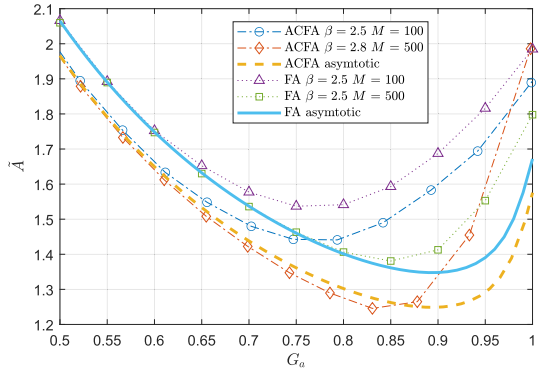

(a) $G1$ sampling method

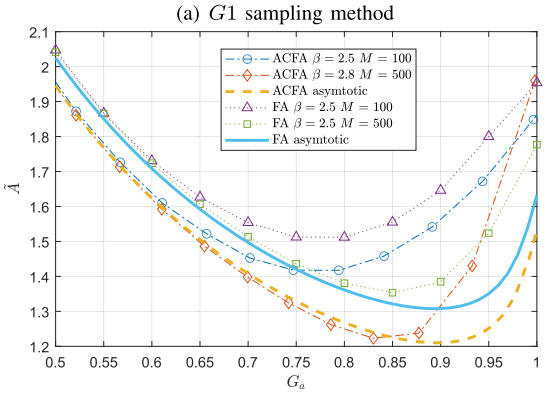

(b) GT sampling method

Fig. 14. The minimum $\tilde{A}_{s,G1}$ and $\tilde{A}_{s,GT}$ versus average system load G_a for frameless ALOHA and ACFA protocol with their own β^* in sparse access model.

Fig. 14 shows the normalized AAoI performance of the FA and ACFA protocols under the optimal β^* for two sampling methods. In both sampling methods, the asymptotic curves of the FA and ACFA protocols can effectively fit the normalized AAoI curve at high frame length. When G_a increases from 0.5 to 0.9, all AAoI curves first decrease due to the high ASP when $G_a < 0.9$ as shown in Fig.7 (a). Then, when G_a is larger than 0.9, under the combined influence of a large number of UEs perform accessing and the access-banned policy, the ASP drops sharply and most UEs cannot complete the update in time, resulting in AAoI also significantly increases. In $G1$ in Fig. 14(a), the ACFA protocol reaches $1.44, 1.24$ at $M = 100, 500$, which is lower than the 1.53 and 1.38 achieved by the FA protocol by 6% and 11%, respectively. Similarly, in GT in Fig. 14(b), the ACFA scheme achieves 1.42 and 1.22, which is 7% and 10% lower than the 1.52 and 1.35 achieved by the FA protocol, respectively. Under the same frame length, the G_a corresponding to the lowest point of the ACFA protocol is also almost the same as that of the FA protocol, but it shifts to the left with the increasing of M. At $M = 100$, the G_a^* of the two schemes are almost 0.75, while in the case of $M = 500$, the G_a^* corresponding to ACFA and FA are 0.83 and 0.85, respectively. We note that the sampling method hardly affects the choice of β^* combined with Fig. 13, so it does not affect the overall trend of the curves (such as G_a^*).

VI. Conclusion

In this paper, we proposed a new policy to reduce the AAoI of the FA protocol. We first proposed two typical access models and AoI sampling methods to establish the basic scenarios. We introduced two aspects of ACFA protocol in detail, i.e., standard FA protocol and access-banned policy. In order to analyze the ASP performance of the ACFA protocol in two access models, we defined some key parameters and proposed two iterative frameworks for ASP analysis in the asymptotic regime, where the results of G_a v.s. η and G_a v.s. ζ can provide an efficient solution for different performance requirements. Subsequently, we derived the closed expressions of AAoI in four scenarios, and established four optimization problem of AAoI, respectively. By solving the above four optimization problem, the choice of the key parameter β^* was given to help adjusting the other parameters, and we showed the normalized AAoI performance of the optimized FA and ACFA protocols. In particular, in the dense access model, we compared with the REARLY-5 scheme, and the simulation results showed that the proposed ACFA protocol outperformed than the existing schemes. Our future work includes extend the access-banned policy to the multiply frames and slots cases to further optimize the energy efficiency, and also can extend our ACFA protocol for a multitype services coexistence scenario.

References

[1] M. Vaezi et al., "Cellular, wide-area, and non-terrestrial IoT: A survey on 5G advances and the road toward 6G," *IEEE Commun. Surveys Tuts.*, vol. 24, no. 2, pp. 1117–1174, 2nd Quart., 2022.

[2] J. Jiao, L. Xu, S. Wu, Y. Wang, R. Lu, and Q. Zhang, "Unequal access latency random access protocol for massive machine-type communications," *IEEE Trans. Wireless Commun.*, vol. 19, no. 9, pp. 5924–5937, Sep. 2020.

[3] Z. Rao, J. Jiao, Y. Wang, S. Wu, R. Lu, and Q. Zhang, "Code-domain collision resolution grant-free random access for massive access in IoT," *IEEE Trans. Wireless Commun.*, early access, Dec. 14, 2022, doi: 10.1109/TWC.2022.3227569.

[4] M. B. Shahab, R. Abbas, M. Shirvanimoghaddam, and S. J. Johnson, "Grant-free non-orthogonal multiple access for IoT: A survey," *IEEE Commun. Surveys Tuts.*, vol. 22, no. 3, pp. 1805–1838, 1st Quart., 2020.

[5] N. Abramson, "The throughput of packet broadcasting channels," *IEEE Trans. Commun.*, vol. COM-25, no. 1, pp. 117–128, Jan. 1977.

[6] A. Mengali, R. De Gaudenzi, and Č. Stefanović, "On the modeling and performance assessment of random access with SIC," *IEEE J. Sel. Areas Commun.*, vol. 36, no. 2, pp. 292–303, Feb. 2018.

[7] C. Stefanovic and P. Popovski, "Coded slotted ALOHA with varying packet loss rate across users," in *Proc. IEEE Global Conf. Signal Inf. Process.*, Dec. 2013, pp. 787–790.

[8] C. Stefanovic, E. Paolini, and G. Liva, "Asymptotic performance of coded slotted ALOHA with multipacket reception," *IEEE Commun. Lett.*, vol. 22, no. 1, pp. 105–108, Jan. 2018.

[9] Z. Chen, Y. Feng, C. Feng, L. Liang, Y. Jia, and T. Q. S. Quek, "Analytic distribution design for irregular repetition slotted ALOHA with multi-packet reception," *IEEE Trans. Veh. Technol.*, vol. 72, no. 1, pp. 1360–1365, Jan. 2023.

[10] S. Salehi and B. Eslamnour, "Improving UAV base station energy efficiency for industrial IoT URLLC services by irregular repetition slotted-ALOHA," *Comput. Netw.*, vol. 199, Nov. 2021, Art. no. 108415.

[11] I. Hmedoush et al., "A regret minimization approach to frameless irregular repetition slotted AlOHA: IRSA-RM," in *Proc. Int. Conf. Mach. Learn. Netw.*, 2020, pp. 73–92.

[12] C. Stefanović, P. Popovski, and D. Vukobratovic, "Frameless ALOHA protocol for wireless networks," *IEEE Commun. Lett.*, vol. 16, no. 12, pp. 2087–2090, Dec. 2012.

[13] F. Lázaro and Č. Stefanović, "Finite-length analysis of frameless ALOHA with multi-user detection," *IEEE Commun. Lett.*, vol. 21, no. 4, pp. 769–772, Apr. 2017.

[14] C. Stefanovic, K. F. Trilingsgaard, N. K. Pratas, and P. Popovski, "Joint estimation and contention-resolution protocol for wireless random access," in *Proc. IEEE Int. Conf. Commun. (ICC)*, Jun. 2013, pp. 3382–3387.

[15] V. Boljanovic, D. Vukobratovic, P. Popovski, and C. Stefanovic, "User activity detection in massive random access: Compressed sensing vs. coded slotted ALOHA," in *Proc. IEEE 18th Int. Workshop Signal Process. Adv. Wireless Commun. (SPAWC)*, Jul. 2017, pp. 1–6.

[16] R. Talak, S. Karaman, and E. Modiano, "Improving age of information in wireless networks with perfect channel state information," *IEEE/ACM Trans. Netw.*, vol. 28, no. 4, pp. 1765–1778, Aug. 2020.

[17] R. D. Yates et al., "Age of information: An introduction and survey," *IEEE J. Sel. Areas Commun.*, vol. 39, no. 5, pp. 1183–1210, May 2021.

[18] S. Kaul, R. Yates, and M. Gruteser, "Real-time status: How often should one update?" in *Proc. IEEE INFOCOM*, Mar. 2012, pp. 2731–2735.

[19] Y. Sun, E. Uysal-Biyikoglu, R. D. Yates, C. E. Koksal, and N. B. Shroff, "Update or wait: How to keep your data fresh," *IEEE Trans. Inf. Theory*, vol. 63, no. 11, pp. 7492–7508, Nov. 2017.

[20] A. Munari and A. Frolov, "Average age of information of irregular repetition slotted ALOHA," in *Proc. IEEE Global Commun. Conf.*, Dec. 2020, pp. 1–6.

[21] A. Munari, "Modern random access: An age of information perspective on irregular repetition slotted ALOHA," *IEEE Trans. Commun.*, vol. 69, no. 6, pp. 3572–3585, Jun. 2021.

[22] H. Asgari, A. Munari, and G. Liva, "On the performance of irregular repetition slotted ALOHA with an age of information threshold," in *Proc. Next Gener. Netw. Appl. Workshop*, 2022, pp. 1–6.

[23] S. Saha, V. B. Sukumaran, and C. R. Murthy, "On the minimum average age of information in IRSA for grant-free mMTC," *IEEE J. Sel. Areas Commun.*, vol. 39, no. 5, pp. 1441–1455, May 2021.

[24] I. Kadota and E. Modiano, "Age of information in random access networks with stochastic arrivals," in *Proc. IEEE INFOCOM Conf. Comput. Commun.*, May 2021, pp. 1–10.

[25] H. Chen, Y. Gu, and S.-C. Liew, "Age-of-information dependent random access for massive IoT networks," in *Proc. IEEE INFOCOM Conf. Comput. Commun. Workshops (INFOCOM WKSHPS)*, Jul. 2020, pp. 930–935.

[26] D. C. Atabay, E. Uysal, and O. Kaya, "Improving age of information in random access channels," in *Proc. IEEE INFOCOM Conf. Comput. Commun. Workshops (INFOCOM WKSHPS)*, Jul. 2020, pp. 912–917.

[27] O. T. Yavascan and E. Uysal, "Analysis of slotted ALOHA with an age threshold," *IEEE J. Sel. Areas Commun.*, vol. 39, no. 5, pp. 1456–1470, May 2021.

[28] X. Chen, K. Gatsis, H. Hassani, and S. S. Bidokhti, "Age of information in random access channels," *IEEE Trans. Inf. Theory*, vol. 68, no. 10, pp. 6548–6568, Oct. 2022.

[29] Y. Huang, J. Jiao, S. Wu, R. Lu, and Q. Zhang, "Age-critical frameless ALOHA protocol for grant-free massive access," in *Proc. IEEE Global Commun. Conf. (GLOBECOM)*, Dec. 2021, pp. 1–6.

[30] C. Stefanović and P. Popovski, "ALOHA random access that operates as a rateless code," *IEEE Trans. Commun.*, vol. 61, no. 11, pp. 4653–4662, Nov. 2013.

[31] T. Akyildiz, U. Demirhan, and T. M. Duman, "Energy harvesting irregular repetition ALOHA with replica concatenation," *IEEE Trans. Wireless Commun.*, vol. 20, no. 2, pp. 955–968, Feb. 2021.

[32] C. Stefanovic, H. M. Gursu, Y. Deshpande, and W. Kellerer, "Analysis of tree-algorithms with multi-packet reception," in *Proc. GLOBECOM IEEE Global Commun. Conf.*, Dec. 2020, pp. 1–6.

[33] C. Stefanovic, F. Lazaro, and P. Popovski, "Frameless ALOHA with reliability-latency guarantees," in *Proc. GLOBECOM IEEE Global Commun. Conf.*, Dec. 2017, pp. 1–6.

[34] F. Lazaro, C. Stefanovic, and P. Popovski, "Reliability-latency performance of frameless ALOHA with and without feedback," *IEEE Trans. Commun.*, vol. 68, no. 10, pp. 6302–6316, Oct. 2020.

[35] F. Lazaro and C. Stefanovic, "Finite-length analysis of frameless ALOHA," in *Proc. 11th Int. ITG Conf. Syst., Commun. Coding*, 2017, pp. 1–6.

[36] Y. Sun, Y. Polyanskiy, and E. Uysal, "Sampling of the Wiener process for remote estimation over a channel with random delay," *IEEE Trans. Inf. Theory*, vol. 66, no. 2, pp. 1118–1135, Feb. 2020.

[37] X. Chen, X. Liao, and S. S. Bidokhti, "Real-time sampling and estimation on random access channels: Age of information and beyond," in *Proc. IEEE INFOCOM Conf. Comput. Commun.*, May 2021, pp. 1–10.

[38] H. M. Gursu, W. Kellerer, and C. Stefanovic, "On throughput maximization of grant-free access with reliability-latency constraints," in *Proc. IEEE Int. Conf. Commun. (ICC)*, May 2019, pp. 1–7.

[39] J. Jiao, L. Xu, S. Wu, R. Lu, and Q. Zhang, "MSPA: Multislot pilot allocation random access protocol for mMTC-enabled IoT system," *IEEE Internet Things J.*, vol. 8, no. 24, pp. 17403–17416, Dec. 2021.

[40] J. Sun, R. Liu, and E. Paolini, "Unrecovered users distribution in coded random access systems with erasures," in *Proc. ICC -IEEE Int. Conf. Commun. (ICC)*, May 2019, pp. 1–6.

Yuhao Huang received the B.S. degree in communication engineering from Hohai University, Nanjing, China, in 2020, and the M.S. degree in electronics and communication engineering from the Harbin Institute of Technology at Shenzhen, Shenzhen, China, in 2022. His research interests include the Internet of Things, massive access, code slotted ALOHA random access, and the age of information.

Jian Jiao (Senior Member, IEEE) received the M.S. and Ph.D. degrees in communication engineering from the Harbin Institute of Technology (HIT), Harbin, China, in 2007 and 2011, respectively. From 2011 to 2015, he was a Post-Doctoral Research Fellow with the Communication Engineering Research Centre, Harbin Institute of Technology Shenzhen Graduate School, Shenzhen, China. From 2016 to 2017, he was a China Scholarship Council Visiting Scholar with the School of Electrical and Information Engineering, The University of Sydney, Sydney, Australia. Since 2017, he has been with the Harbin Institute of Technology at Shenzhen (HITSZ), where he has been a Professor with the Guangdong Provincial Key Laboratory of Aerospace Communication and Networking Technology since 2022. He is currently an Associate Professor with the Peng Cheng Laboratory, Shenzhen. His current research interests include semantic communications, satellite communications and networking, and coding techniques. He is serving as the Editor for *Science China Information Sciences*.

Ye Wang (Member, IEEE) received the M.S. and Ph.D. degrees in information and communication engineering from the Harbin Institute of Technology (HIT), Harbin, China, in 2009 and 2013, respectively. From 2013 to 2014, he was a Post-Doctoral Research Fellow with the University of Ontario Institute of Technology, Canada. From 2015 to 2021, he was an Assistant Professor with the Harbin Institute of Technology at Shenzhen (HITSZ). Since 2022, he has been an Associate Professor with the Peng Cheng Laboratory, Shenzhen. His research interests include satellite communications, resource allocation, and mobile Internet.

Xingjian Zhang (Member, IEEE) received the B.Sc. degree (Hons.) in telecommunications engineering from the Beijing University of Posts and Telecommunications, Beijing, China, in 2014, and the Ph.D. degree in electronic engineering from the Queen Mary University of London, London, U.K., in 2018. He is currently an Assistant Professor with the Department of Electronics and Information Engineering, Harbin Institute of Technology at Shenzhen (HITSZ). His research interests include satellite-based wideband spectrum sensing, radio frequency spectrum learning, distributed optimization, and compressive sensing.

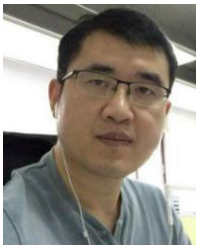

Shaohua Wu (Member, IEEE) received the Ph.D. degree in communication engineering from the Harbin Institute of Technology (HIT), Harbin, China, in 2009. From 2009 to 2011, he was a Post-Doctoral Researcher with the Department of Electronics and Information Engineering, Shenzhen Graduate School, Harbin Institute of Technology at Shenzhen (HITSZ), Shenzhen, China, where he was an Associate Professor from 2012 to 2020. Since 2021, he has been a Professor with the School of Electrical and Information Engineering, HITSZ, and a Professor with the Peng Cheng Laboratory, Shenzhen. His current research interests include wireless image/video transmission, space communications, advanced channel coding techniques, and B5G wireless transmission technologies.

Rongxing Lu (Fellow, IEEE) received the Ph.D. degree from the Department of Electrical and Computer Engineering, University of Waterloo, Canada, in 2012. He is currently the Mastercard IoT Research Chair, a University Research Scholar, and an Associate Professor with the Faculty of Computer Science (FCS), University of New Brunswick (UNB), Canada. Before that, he was an Assistant Professor with the School of Electrical and Electronic Engineering, Nanyang Technological University (NTU), Singapore, from April 2013 to August 2016. He was a Post-Doctoral Fellow with the University of Waterloo from May 2012 to April 2013. His research interests include applied cryptography, privacy enhancing technologies, and the IoT-big data security and privacy. He has published extensively in his areas of expertise. He was awarded the most prestigious Governor General's Gold Medal in his Ph.D. study and won the 8th IEEE Communications Society (ComSoc) Asia Pacific (AP) Outstanding Young Researcher Award in 2013. He was a recipient of nine best (student) paper awards from some reputable journals and conferences. He was the Winner of the 2016–2017 Excellence in Teaching Award, FCS, UNB. He serves as the Chair for the IEEE ComSoc Communications and Information Security Technical Committee (CIS-TC) and the Founding Co-Chair for the IEEE TEMS Blockchain and Distributed Ledgers Technologies Technical Committee (BDLT-TC).

Qinyu Zhang (Senior Member, IEEE) received the bachelor's degree in communication engineering from the Harbin Institute of Technology (HIT) in 1994 and the Ph.D. degree in biomedical and electrical engineering from the University of Tokushima, Japan, in 2003. From 1999 to 2003, he was an Assistant Professor with the University of Tokushima. He has been with the Harbin Institute of Technology at Shenzhen (HITSZ) since 2003, where he is currently a Full Professor and the Vice President. His research interests include aerospace communications and networks, and wireless communications and networks. He has been awarded the National Science Fund for Distinguished Young Scholars, the Young and Middle-Aged Leading Scientist of China, and the Chinese New Century Excellent Talents in University, and received three scientific and technological awards from governments.